Original Article

MOLECULAR METABOLISM

Sodium-glucose co-transporter2 expression and inflammatory activity in diabetic atherosclerotic plaques: Effects of sodium-glucose co-transporter2 inhibitor treatment

Nunzia D'Onofrio [1,10], Celestino Sardu [2,10], Maria Consiglia Trotta [3], Lucia Scisciola [2], Fabrizio Turriziani [2], Franca Ferraraccio [4], Iacopo Panarese [4], Lella Petrella [5], Mara Fanelli [6], Piero Modugno [7], Massimo Massetti [6], Ludovica Vittoria Marfella [1], Ferdinando Carlo Sasso [2], Maria Rosaria Rizzo [2], Michelangela Barbieri [2], Fulvio Furbatto [7], Fabio Minicucci [7], Ciro Mauro [7], Massimo Federici [8], Maria Luisa Balestrieri [1], Giuseppe Paolisso [2,9,11], Raffaele Marfella [2,8,*,11]

ABSTRACT

Objective: We evaluated sodium-glucose co-transporter2 (SGLT2) expression and the effect of SGLT2 inhibitor (SGLT2i) therapies on carotid plaques of asymptomatic diabetic and non-diabetic patients.

Methods: Plaques were obtained from 296 non-diabetic patients and 227 patients with type 2 diabetes undergoing carotid endarterectomy. 97 patients with type 2 diabetes were treated with SGLT2 inhibitors for 16 $\pm$ 4 months before endarterectomy. After propensity score matching analysis, patients with type 2 diabetes were categorized without (n = 87) and with SGLT2i therapy (n = 87). To investigate SGLT2 expression levels' effects on major adverse endpoints (MACE = stroke, transient ischemic attack, myocardial infarction, and death), we evaluated MACE outcomes at a 2-year follow-up.

Results: Compared to plaques from patients without diabetes, plaques from patients with diabetes had higher SGLT2 expression, inflammation, and oxidative stress, along with lower SIRT6 expression and collagen content. Compared with plaques from patients with diabetes, SGLT2i-treated patients with type 2 diabetes presented increased SIRT6 expression and collagen content and lowered inflammation and ion and oxidative stress, thus indicating a more stable plaque phenotype. These results supported in vitro observations on human aorta endothelial cells (EC) (TeloHAEC-cells). Indeed, EC treated with high glucose (25 mM) in the presence of SGLT2i (100 nM canagliflozin) presented higher SIRT6 expression and decreased mRNA and protein SGLT2 levels, nuclear factor-kappa B (NF-B(NF $-$ κB), and matrix metallopeptidase 9 (MMP-9) expression compared to cells treated only with high glucose. After two years following endarterectomy, a multivariable Cox regression analysis showed significantly higher 2-year overall survival from MACE in patients without diabetes ($P < 0.01$). Among patient with diabetes, the current SGLT2i users presented a significantly lower rate of MACE through 2 years compared to non-SGLT2i users ($P < 0.05$).

Conclusions: These findings unveil a critical involvement of the SGLT2/SIRT6 pathway in the inflammatory process of diabetic atherosclerotic lesions and suggest its possible favorable modulation by SGLT2i.

Keywords Atherosclerosis; Type 2 diabetes mellitus; SGLT2; Sirtuin-6; Inflammation

[1]Department of Precision Medicine, the University of Campania "Luigi Vanvitelli,", Italy [2]Department of Advanced Medical and Surgical Sciences, University of Campania "Luigi Vanvitelli,", Italy [3]Department of Experimental Medicine, Section of Pharmacology, University of Campania "Luigi Vanvitelli,", Italy [4]Department of Mental Health and Public Medicine, Section of Statistic, the University of Campania "Luigi Vanvitelli,", Naples, Italy [5]Laboratory of Molecular Oncology, Gemelli Molise SpA, Campobasso, Italy [6]Department of Cardiovascular Medicine, Gemelli Molise SpA, Campobasso, Italy [7]Department of Cardiology, Hospital Cardarelli, Naples, Italy [8]Department of Systems Medicine, University of Rome Tor Vergata, Rome, Italy [9]Mediterranea Cardiocentro, Naples, Italy

[10] Share first authorship.

[11] Share last authorship.

*Corresponding author. Piazza Miraglia 2, 80138, Napoli, Italy. Fax: +39 081 5665303. E-mail: raffaele.marfella@unicampania.it (R. Marfella).

Received May 31, 2021 • Revision received August 25, 2021 • Accepted September 2, 2021 • Available online 7 September 2021

https://doi.org/10.1016/j.molmet.2021.101337

1. INTRODUCTION

Cardiovascular disease is the leading cause of death in patients with type 2 diabetes [1]. Diabetes leads to increased vulnerability for plaque disruption and mediates increased incidence and severity of clinical events [2,3]. Sodium-glucose cotransporter 2 inhibitors (SGLT2i] are a newly identified class of antidiabetic drugs that act on proximal renal tubules to decrease glucose reabsorption and promote glucose excretion via the urinary system [4]. The SGLT2i anti-hyperglycemic effects are independent of insulin secretion in patients with diabetes mellitus [5]. Besides their impact on blood glucose, SGLT2i were reported to have other beneficial effects on diabetes patients. As the drugs mainly target proximal renal tubules, there is much literature describing the renal protective effects of SGLT2i [6]. Moreover, it was confirmed that treatment with SGLT2i results in weight loss and reduced risk of cardiovascular diseases, including heart failure and high blood pressure, and improved insulin resistance, lipid profiles, and visceral adiposity [7]. SGLT2 mRNA and protein expression has been reported in murine vascular tissue and endothelial cells in vitro [8]. Additionally, endothelial SGLT2 protein upregulation promotes atherosclerosis progression by reducing [9] sirtuin pathways and increases [10] the inflammatory process by raising the expression of inflammatory molecules such as proinflammatory cytokines. Finally, endothelial SGLT2 protein upregulation decreases atherosclerotic plaque stability by reducing the TIMP-1/MMP-2 ratio expression in animal models [11]. *In vitro* studies demonstrated that high glucose upregulates SGLT2 expression in endothelial cells [12] and that SGLT2i blunts the development and progression of atherosclerosis in animal models [13]. Nevertheless, the fundamental pathological basis of endothelial SGLT2 expression and the effects of SGLT2i on atherosclerotic plaque progression in patients with type 2 diabetes have not been thoroughly elucidated. Here, we aimed to investigate whether diabetes might alter sirtuin-mediated anti-inflammatory activity, thus enhancing atherosclerotic plaques' inflammatory potential and favoring their instability via altered expression of endothelial SGLT2. To this end, this study was designed to identify differences in endothelial SGLT2 expression and inflammatory plaque burden expression between carotid plaques of asymptomatic diabetic and non-diabetic patients. Experimental studies suggested that SGLT2i-based therapies may reduce inflammation and enhance sirtuin pathways [10]. Since we evidenced the involvement of SIRT6 in the inflammatory pathways of diabetic atherosclerotic lesions [14], we evaluated the effects of SGLT2i therapy on SIRT6 expression in carotid plaques of the patient with diabetes and human aorta endothelial cells (EC). Furthermore, a set of in vitro experiments on EC was designed to evaluate the effects of SGLT2i on the SIRT6/inflammatory pathway during high-glucose treatment. Finally, we assessed the impact of SGLT2i in asymptomatic carotid stenosis patients concerning stroke, myocardial infarction, and death, both in the periprocedural period and after a 2-year follow-up.

2. RESEARCH DESIGN AND METHODS

Consecutive patients from the Department of Cardiology and Cardiovascular Surgery of the Cardarelli Hospital, Naples, Italy, and Department of Cardiovascular Medicine, Gemelli Molise SpA, Campobasso, Italy, from January 2016 to December 2020 were recruited for the prospective observational study, in which patients were not randomized in the groups. The subjects were observed to determine their outcome. Among them, we selected 296 patients without diabetes (non-diabetic group) and 227 patients with diabetes with asymptomatic carotid stenosis (according to North American Symptomatic Carotid Endarterectomy Trial classification) who were enlisted to undergo carotid endarterectomy for extracranial high-grade (>70%) internal carotid artery stenosis [15]. Asymptomatic patients underwent a baseline clinical examination and medical history to ensure they had never developed neurologic symptoms or cerebral lesions assessed by computed tomography. All patients received computed tomography or MRI. Diabetes was categorized according to the American Diabetes Association criteria [16]. Additionally, patients with diabetes answered a specific questionnaire about medicines used for diabetes treatment before the beginning of the study, the dates of the beginning and end of therapy, route of administration, and duration of use. Information from this questionnaire and the medicine inventory from the research were used to classify the subjects. The diabetic patients who had never used SGLT2i were classified as "never SGLT2i users," while those who had already used SGLT2i were classified as "current SGLT2i users." The current SGLT2i users were patients who had used SGLT2i for at least six months. Patients treated with SGLT2i for less than 6 months were excluded from the study information regarding the duration that treatment was available for current users. Patients with clinical or laboratory evidence of heart failure, previous stroke, valvular defects, malignant neoplasms, or secondary causes of hypertension were enrolled in the study (exclusion criteria). Carotid sonography was performed on a single ultrasound machine (Aloka 5500). After discharge, the patients were followed quarterly for 24 months. During the visits, all patients underwent clinical and instrumental evaluation. Diabetic patients were also managed for blood glucose and HbA1c levels as well as for dietary intake. The study was approved by the ethics committee and informed written consent was obtained for each patient. The study was approved by the local Ethics Review Committee (n. p. 440).

Laboratory analysis. After an overnight fast, plasma glucose, HbA1c, and serum lipids were measured by enzymatic assays in the hospital's chemistry laboratory. Fasting blood glucose levels were evaluated before surgery. Fasting and postprandial plasma glucose data were obtained from the average of each assessment.

Atherectomy specimens. After surgery, the specimens were cut perpendicular to the long axis into two halves. The first half was frozen in liquid nitrogen. A portion of the other half-specimen was immediately immersion-fixed in 10% buffered formalin. Sections were serially cut at 5 μm, mounted on lysine-coated slides, stained with hematoxylin and eosin, and put through the trichrome method. Carotid artery specimens were analyzed by light microscopy, confocal laser-scanning microscopy, and biochemical assay.

Immunohistochemistry. After the surgical procedure, atherectomy specimens were immediately frozen in isopentane and cooled in liquid nitrogen. Similar regions of plaque were analyzed (Supplementary Figure 1). Serial sections were incubated with the following specific antibodies: anti-CD68 (cluster of differentiation 68 glycoproteins) macrophages, anti-matrix metalloproteinase-9 (MMP-9) (Santa Cruz), proteases involved in the degradation of the collagen content in the plaque, and anti-tumor necrosis factor (TNF)-α (R&D). Analysis of immunohistochemistry was performed by a personal computer-based quantitative 24-bit color image analysis system (IM500; Leica Microsystem AG) [17,18].

Sirius red staining for collagen content. Sections were stained as previously described [19]. After dehydration, the sections were placed on coverslips and observed under polarized light. The sections were photographed with identical exposure settings.

Confocal laser-scanning microscopy. SGLT2 and SIRT6 levels were determined in atherosclerotic plaque sections from patients who were

diabetic, non-diabetic, and diabetic under SGLT2i treatment as well as on endothelial cells. For tissue preparation, antigen retrieval buffer (10 mM Sodium citrate, 0.05% Tween 20, pH 6.0) was added to deparaffinized and rehydrated sections. Slides were then washed in phosphate-buffered saline (PBS) following by incubation with blocking solution for 1 h at room temperature (RT) in fetal bovine serum (FBS) with saponin (0.1 g/mL) and then stained with specific primary and secondary antibodies. Sections were then quenched for auto-fluorescence using the Vector TrueVIEW Autofluorescence Quenching Kit (VEC-SP-8500, Vector Laboratories, catalog no.VEC-SP-8500—15). Negative controls were created by incubating sections from diabetic, nondiabetic, and diabetic SGLT2i-user patients with blocking solution supplemented with a non-immune immunoglobulin IgG antibody instead of specific primary antibodies.

Immunofluorescence analysis on EC, seeded in 24-well plates containing microscope glass, was performed by incubation for 20 min with 4% (v/v) paraformaldehyde solution followed by permeabilization for 10 min with 0.1% (v/v) Triton X-100 in PBS. The primary antibodies anti-SGLT2 (1:500, ab37296, Abcam), anti-SIRT6, (1:500, ab191385, Abcam) and NF-B(NF − κB) (1:1000, ab 16,502, Abcam) were incubated overnight at 4°C on EC or deparaffinized atherosclerotic plaque tissues, followed by 1 h of incubation with Alexa Fluor 633 (1:1000, Life Technologies, Carlsbad, CA, USA). For EC and plaque samples, cytoskeleton staining was performed using antibodies anti-vimentin (1:1000, 5741, Cell Signaling Technology) or von Willebrand factor (1:1000, ab6994, Abcam), respectively, followed by incubation with Alexa Fluor 488 (1:1000, Life Technologies, Carlsbad, CA, USA). For all fluorescence preparations, nuclear staining was performed using 2.5 μg/mL of 4′, 6-diamidino-2-phenylindole (DAPI, Sigma Aldrich, St. Louis, MO, USA) for 7 min. Microscopy analyses were performed using an LSM 700 confocal microscope (Zeiss, Oberkochen, Germany) with a plan apochromat X63 (NA1.4) oil immersion objective. The fluorescence intensity was evaluated by ImageJ 1.52n software (National Institutes of Health, Bethesda, MD, USA) and data expressed as arbitrary fluorescence units (AFU).

Biochemical assays. For preparation of atherosclerotic plaque extracts, 400 mL of 2D lysis buffer (7 mol/L urea, 2 mol/L thiourea, 4% CHAPS [3-([3-cholamidopropyl] dimethylammonium)-1-propane sulfonate] buffer, 30 mmol/L Tris—HCl, pH 8.8) were added to 200 mg of tissues cut into small pieces. Tissue homogenized with a Precellys 24 system (Bertin Technologies) was centrifuged at 800×*g* for 10 min at 4°C to collect the supernatant. Proteins were then precipitated by adding 100% cold methanol. 40 μg of each sample were loaded, electrophoresed in polyacrylamide gel, and electroblotted onto a nitrocellulose membrane. Each determination was repeated at least three times. MMP-9, TNF-α, and nitrotyrosine levels were quantified in plaques using a specific ELISA kit (Santa Cruz, R&D Systems, and Imgenex). NF-B(NF − κB) binding to κB sites was assessed on nuclear extracts from plaque specimens by the Trans-AM NF-B(NF − κB) p65 transcription factor assay kit (Active Motif Europe; Rixensart).

2.1. Real-time reverse transcription polymerase chain reaction (qRT-PCR)

Total RNA isolation from atherosclerotic plaques and human aorta endothelial cells was performed using the RNeasy Mini kit (74,106, Qiagen) according to manufacturer's protocols. RNA purity and concentration were evaluated by the NanoDrop 2000c Spectrophotometer (Thermo Fisher Scientific). The elimination of genomic DNA contamination and the subsequent reverse transcription of mRNA to cDNA was performed using the QuantiTect Reverse Transcription kit (205,311, Qiagen) and the Gene AMP PCR System 9700 (Applied Biosystems). cDNA was amplified with QuantiTect SYBR Green PCR Kit (204,143, Qiagen) and CFX96 Real-time System C1000 Touch Thermal Cycler (Biorad). Specific QuantiTect Primer Assays were used to detect the levels of SLC5A2, encoding SGLT2 (QT00075901, Qiagen) and GAPDH (QT00079247, Qiagen). Gene expression was quantized with the $2^{-\Delta\Delta Ct}$ method.

2.2. Cell culture and treatments

The human aorta endothelial cells (EC) (TeloHAEC cell line, CRL-4052, Lot# 70027940) were grown in an adherent culture and maintained in Vascular Cell Basal Medium (PCS-100—030) supplemented with Endothelial Cell Growth kit-VEGF (PCS-100—041). Cells, medium, and culture kits were purchased from ATCC (American Type Culture Collection, Manassas, VA, USA). Cells were cultured in an incubator at 37°C under a humidified atmosphere with 5% CO_2. The SGLT2i, canagliflozin, under the commercial name of Invokana, was provided by Janssen Pharmaceuticals. An inhibitor stock solution of 224.96 μM was obtained by chopping a 100 mg pill and dissolving it in 1 mL of Hanks' balanced salt solution (HBSS) with 10 mM Hepes. SGLT2i treatments were performed with concentrations ranging from 0.25 μM to 10 μM for up to 24 h. Exposure to high glucose (hGluc) was performed by incubating endothelial cells with 25 mM glucose for 48 h. For the combined treatment (SGLT2i+hGluc), EC were pre-treated for 8 h with SGLT2i and then washed with PBS before being exposed to hGluc for 48 h. Control cells (Ctr) were maintained in a complete culture medium with normal glucose concentration and corresponding volumes of HBSS-10 mM Hepes. Osmotic control was performed by treatment with 25 mM L-glucose.

Measurement of cell viability and cytotoxicity. EC viability was detected by Cell Counting Kit-8 (CCK-8 Donjindo Molecular Technologies, Inc., MD, USA) following the manufacturer's instructions, as previously described [14]. Briefly, CCK-8 solution (10 μL) was added to each well and then plated and incubated for 4 h at 37°C. After that, absorbance was measured at 450 nm with microplate reader model 680 Bio-Rad. All experiments were performed with n = 5 replicates, and cell viability was expressed as the mean of the optical density at 450 nm ± Standard Deviation (SD). To assess the cell membrane's integrity, the release of lactate dehydrogenase (LDH) into the medium by Cytotoxicity LDH Assay Kit-WST (Dojindo, CK12) was measured. According to the manufacturer's instructions, after treatments, 100 μL of the working solution was added to 50 μL of endothelial cell suspension and then plate incubated and protected from light at room temperature for 30 min. The absorbance was measured with microplate reader model 680 Bio-Rad at 490 nm, and the following equation was used to calculate the cytotoxicity (%): (Test Substance − Low Control)/(High Control − Low Control) x 100.

Transient SIRT6 and SGLT2 silencing. Transient transfection was performed with small interfering RNA (siRNA) (40 nM), consisting of three SIRT6-siRNA oligos (NM_016,539) or an SGLT2-siRNA oligos set (NM_003041) from Applied Biological Materials (Inc. Richmond, BC, Canada), with a non-targeting siRNA (Scramble siRNA) (40 nM) as control, using RNAifectin transfection reagent. EC were seeded in a 6-well culture plate (5.0 × 105 cells/well) in a complete medium. After 24 h, cells were incubated with siRNA-RNAifectin complexes dissolved in serum- and antibiotic-free medium for 16 h before starting treatments.

Cell lysis and Western blotting analysis. EC were washed with PBS and immediately scraped off the plate in lysis buffer (1% NP-40, 0.5% sodium deoxycholate, 0.1% SDS in PBS containing 10 μg/mL aprotinin, leupeptin, and 1 mM phenylmethylsulfonyl fluoride, PMSF). After

30 min of gentle shaking at 4°C, scraped cells were sonicated and centrifuged at 12000 × *g* for 10 min. Supernatants were collected, and the total protein concentration of each extract was determined by the Bio-Rad Protein Assay kit (Bio-Rad, Hercules, CA). Protein extracts (40–60 μg) were subjected to sodium dodecyl sulfate-polyacrylamide gel electrophoresis (SDS-PAGE) and transferred to nitrocellulose membranes with a Trans-Blot Turbo Transfer System (BioRad). Membranes were blocked in 10 mM Tris–HCl, pH 8.0, 150 mM NaCl, 0.05% Tween 20 (TBST) supplemented with 5% nonfat dry milk for 1 h at room temperature and then incubated overnight at 4°C with specific primary antibodies anti-SIRT6 (1:1000, Abcam, ab191385), anti-SGLT2 (1:1000, #14210, Cell Signaling Technology), anti-SGLT2 (1:600, 24654-1-AP, Proteintech), anti-SGLT2 (1:500, PA5-59644, Thermo Fisher Scientific), anti-SGLT2 (1:500, ab37296, Abcam), anti-NF-kB (1:1000, Abcam, ab16502), anti-MMP-9 (1:1000, Abcam, ab58803), and anti-TNF-α (1:1000, ab6671, Abcam). Anti-α-tubulin (1:5000, E-AB-20036, Elabscience), anti-β-actin (1:5000, #3700, Cell Signaling Technology), and GAPDH (1:10.000, ab9485, Abcam) were used as the loading control. SGLT1 Blocking Peptide (1:200, #BLP-GT031, alomone labs) was preincubated (2 h at room temperature) before the addition of anti-SGLT2 primary antibody to investigate the cross reactivity between SGLT1 and SGLT2 antigens.

After 1 h of incubation with HRP-conjugated secondary antibodies (NC GxMu-003-DHRPX and GtxRb-003-DHRPX, ImmunoReagents Inc.), immunocomplexes were detected by Excellent chemiluminescent substrate (Elabscience, E-IR-R301) and visualized by using ChemiDoc Imaging System with Image Lab 6.0.1 software (Bio-Rad Laboratories). The densities of immunoreactive bands were measured with ImageJ 1.52n software (National Institutes of Health) and expressed as arbitrary units (AU) [20].

Extracellular reactive oxygen species (ROS) measurement. The amount of extracellular H_2O_2 released from EC after treatments were measured with the Amplex Red Hydrogen Peroxide/Peroxidase Assay Kit (Thermo Fisher Scientific, A22188. A 2 × 104 suspension of live cells in Krebs–Ringer phosphate glucose buffer (145 mM NaCl, 5.7 mM sodium phosphate, 4.86 mM KCl, 0.54 mM $CaCl_2$, 1.22 mM $MgSO_4$, 5.5 mM glucose, pH 7.35) was mixed with 100 μL Amplex Red reagent containing 50 μM Amplex Red and 0.1 U HRP/mL. After incubation at 37°C for 60 min, the fluorescence was measured using a Tecan Infinite 2000 Multiplate reader at an excitation wavelength of 530 nm and an emission wavelength of 590 nm. Extracellular ROS content was calculated by comparing the fluorescence of each sample to an H_2O_2 standard curve.

Detection of intracellular ROS. Intracellular ROS levels were determined by staining with the fluorescent probe 2′,7′-dichlorodihydrofluorescein diacetate (DCFH-DA, D6883, Sigma–Aldrich) following the manufacturer's instructions. After treatment, EC were incubated for 1 h with 10 μM DCFH-DA in the dark at 37°C. Subsequently, cells were detached, harvested, and washed twice with PBS. The DCF fluorescence intensity was quantified using a BD Accuri C6 cytometer. Menadione (50 μM) was used as a positive control [21].

Mitochondrial ROS assessment. Mitosox Red Mitochondrial Superoxide Indicator (Thermo Scientific, M36008) was used to selectively detect the superoxide levels spread by mitochondria following the manufacturer's protocols. After treatment, EC were stained with 5 μM Mitosox for 20 min at 37°C. Cells were harvested and washed in PBS. Then, the median fluorescence intensity (MFI) was quantified using a BD Accuri C6 cytometer. Data were analyzed by FlowJo V10 software. Mitochondrial ROS evaluation by Mitosox Red staining was also carried out on EC, which was seeded in a 24-well plate containing microscope glass for confocal laser microscopy detection. After probe incubation on live cells, samples were fixed with paraformaldehyde and then processed as reported under the "Confocal laser scanning microscopy" paragraph. The cytoskeleton was marked with Phalloidin-iFluor 488 (1:1000, ab176753, Abcam), while DAPI was used for nuclei counterstaining. Menadione (50 μM) was used as a positive control.

Evaluation of cytokine levels. The assessment of cytokine levels (IL-6, IL-8, TNF-α, and monocyte chemoattractant protein 1, MCP-1) was performed with specific ELISA assays (human interleukin-6 ELISA, BioVendor, RD194015200R; human interleukin-8, BioVendor, RD194558200R; ELISA Cymax TNF-alpha ELISA, YIF-LF-EK0193; human MCP-1 ELISA, BioVendor, RAF081R, respectively) according to the manufacturer's protocols. After treatment, EC lysates were incubated in microplate wells pre-coated with specific anti-cytokine antibodies. After 1 h of incubation, cells were washed to remove unbound cytokines. Biotin-labeled anti-IL-6, -IL-8, -TNF-α, and -MCP-1 antibodies were then added and incubated for 1 h. After washing, streptavidin-HRP conjugate was added and set for 30 min. The absorbance was measured at 450 nm using a microplate reader model 680 Bio-Rad, and cytokine levels were estimated by plotting sample absorbance values against standard curves for each analyzed cytokine.

Statistical analysis. SPSS version 23.0 (IBM statistics) was used for all statistical analyses. Categorical variables were presented as frequencies (percentages) and continuous variables as mean ± SD. The normal distribution of data was evaluated with the Kolmogorov Smirnov test, and a parametric test was used. For comparison among diabetic never SGLT2i users and current SGLT2i users, propensity score matching (PSM) was developed from the predicted probabilities of a multivariable logistic regression model predicting mortality and events from age, sex, hypertension, dyslipidemia, smoking history, family history, baseline no-diabetic therapies, metabolic parameters, and cardiovascular diseases. In all matched patients, the balancing property was satisfied. To investigate SGLT2 expression levels' effects on major adverse endpoints (MACE = stroke, transient ischemic attack, myocardial infarction, and death), we evaluated MACE outcomes at a 2-year follow-up stratified by SGLT2 expression tertiles. Regression analysis was performed to estimate the relationships among variables. A sample size of 207 patients and 17 events was considered sufficient to determine a hazard ratio of 0:31 to detect the comparison between groups with a power of 80% and a significance level of 5%. We thus performed appropriate Cox regression models that were then used to compare event risks. The resulting hazard ratios (HRs) and 95% CIs were reported. All in vitro reported results refer to experiments performed at least three times. Statistical differences were assessed by repeated measures, mixed model analysis, and one-way ANOVA followed by Bonferroni's posthoc tests. Two-tailed P values < 0.05 were considered statistically significant. All analyses were performed with SPSS software version 243.0 (IBM statistics), and STATA 15.5 (StataCorp. 2019. College Station, TX: StataCorp LLC) was used for all statistical analyses.

Data and Resource Availability: The datasets generated and analyzed during the current study are available from the corresponding author upon reasonable request. After manuscript publication, the datasets generated and analyzed during the current study will be available at the ClinicalTrials.gov site, number NCT03962686.

3. RESULTS

3.1. Patient characteristics

A total of 523 consecutive patients with asymptomatic carotid stenosis (according to North American Symptomatic Carotid Endarterectomy Trial classification) [22] enlisted to undergo carotid endarterectomy for

extracranial high-grade (>70%) internal carotid artery stenosis were evaluated. Because of advanced atherosclerosis lesions (carotid plaque stenosis >70%), all patients were treated with antiplatelet agents, blood pressure medications, and statins for at least 1 year, without differences between the groups. Of these, 296 patients were non-diabetic (non-diabetic group) and 227 patients were diagnosed with type 2 diabetes (Table 1). Among the 227 patients with diabetes enrolled in the study, 130 were never SGLT2i users, and 97 were current SGLT2i users; after PSM for metabolic and nondiabetic therapies and cardiovascular risk factors, 87 never SGLT2i users were matched to 87 current SGLT2i users (Supplementary Table). The duration of SGLT2i treatment was 26 ± 8 months (mean ± SD). The SGLT2i drugs were added to the previous antidiabetic therapy as reported in the Supplementary Table. The duration of previous antidiabetic therapy was almost 10 years, without differences among the groups (current SGLT2i users, 13 ± 2 years; never SGLT2i users, 12 ± 4 years).

In-hospital treatments and glucose control. In patients with diabetes, the mean, fasting, and postprandial plasma glucose levels at baseline and during the week before the surgery as well as HbA1c (A1C) levels did not differ among never SGLT2i users and current SGLT2i users (Supplementary Table). During hospitalization, patients were treated according to the most recent international guidelines [23], with high proportions of patients receiving platelet inhibitors and antithrombotic agents before, during, and after the procedure. In particular, aspirin was administered to 98% and statins to 86% of patients in both groups. Beta-blockers were given to 81% of patients, of whom 43% received an ACE inhibitor in both groups. Among the whole study population, 88% of patients were treated with a combination therapy of thienopyridine and aspirin. Before the intervention, oral antidiabetic therapy was discontinued for patients with diabetes. All patients with diabetes were treated with insulin therapy as basal/bolus administration until 3 days post-intervention. The mean blood glucose and units of insulin were not different among the groups (data not shown). At hospital discharge, fasting and postprandial plasma glucose levels were: fasting, 133 ± 31 mg/dL; postprandial, 177 ± 19 mg/dL, without significant difference between never SGLT2i users and current SGLT2i users.

Treatments at 2 years following discharge. Over the 2-year follow-up period, there was no difference in cardiovascular therapies between the groups. Patients with diabetes did not show any significant difference in metabolic control compared to groups in the overall population. During the 2-year follow-up, there were no differences in glycemic control among never SGLT2i users and current SGLT2i users (Supplementary Figure 2). During the follow-up, we observed a significant drop in HbA1c in both groups (−1.5 ± 0.3% in current SGLT2i users and −1.6 ± 0.5 in never SGLT2i users). The good glycemic control obtained during the follow-up may be due to the strict management of the patients, which was carried out quarterly. The drop in HbA1c was in accord with standards of medical care in diabetes [16]. During the 2-year follow-up, there were no differences in dietary interventions between the groups.

Table 1 — Characteristics of study patients.

Patients characteristics	*Non diabetic patients (N = 296)*	*Diabetic patients (N = 227)*	*P*
Age, years	65.1 ± 5.9	65.2 ± 5.9	0.910
Sex male, n (%)	187 (63.2)	140 (61.2)	0.223
Heart rate, batt/min	81 ± 10	82 ± 8	0.088
Hypertension, n (%)	101 (34.1)	157 (69.2)	0.001
Dyslipidemia, n (%)	108 (36.5)	128 (56.4)	0.001
Cigarette smoking, n (%)	41 (13.9)	23 (10.1)	0.227
Heart disease, n (%)	101 (34.1)	99 (43.6)	0.017
BMI, kg/m^2	26.5 ± 2.0	28.5 ± 1.9	0.001
Systolic blood pressure, mmHg	125 ± 11	127 ± 9	0.017
Diastolic blood pressure, mmHg	77 ± 6	79 ± 7	0.001
HbA1C, %	5.5 ± 0.8	8.5 ± 0.8	0.001
Blood glucose, mg/dl	105 ± 16	201 ± 25	0.001
Total cholesterol, mg/dl	186 ± 29	208 ± 25	0.001
HDL cholesterol, mg/dl	40 ± 3	37 ± 3	0.001
LDL cholesterol, mg/dl	115.7 ± 19	136.7 ± 16	0.023
Triglycerides, mg/dl	158 ± 21	184 ± 24	0.001
Creatinine, mg/dl	1 ± 0.1	1.1 ± 0.1	0.195
Plaque characteristics			
Stenosis severity, %	74.7 ± 4.6	75.1 ± 4.7	0.336
Active therapy			
Aspirin, n (%)	255 (86.1)	205 (90.3)	0.175
Warfarin, n (%)	25 (8.4)	20 (8.8)	0.454
β-Blocker, n (%)	187 (63.2)	99 (43.6)	0.001
Calcium-channel blocker, n (%)	40 (13.5)	25 (11)	0.424
Statin, n (%)	270 (91.2)	211 (93)	0.519
ACE inhibitor, n (%)	109 (36.8)	96 (42.3)	0.207
Diuretic agent, n (%)	35 (11.8)	14 (6.2)	0.033
AT-2 antagonist, n (%)	119 (40.2)	79 (37.9)	0.237

Data are presented as mean ± SD, or number (%). IHD = ischemic heart disease; BMI = body mass index; HbA1c = Hemoglobin A1c; HDL = high-density lipoprotein; LDL = low-density lipoprotein; SGLT2 = Sodium-glucose co-transporter-2; SIRT6 = sirtuin 6; ACE = angiotensin-converting enzyme; AT2 = Angiotensin 2.

3.2. Plaque composition

Confocal laser-scanning microscopy revealed that levels of SIRT6 expression were consistently lower in plaques from patients with type 2 diabetes compared to plaques from patients without diabetes ($P < 0.01$) (Figure 1 A, B and Supplementary Figure 3). Treatment with SGLT2i showed a consistent upregulation of SIRT6 expression compared to diabetic subjects ($P < 0.05$). In contrast, we observed an upregulation of SGLT2 expression in diabetic compared to nondiabetic specimens ($P < 0.01$), which resulted in downregulation by SGLT2i treatment ($P < 0.05$). Colocalization of SIRT6/SGLT2 and von Willebrand factor showed that SIRT6 and SGLT2 were expressed by endothelial cells (Figure 1 A and B). These results were confirmed by Western blot analysis showing decreased levels of SIRT6 in atherosclerotic plaques from diabetic compared to non-diabetic patients (P<0.01) and increased levels in current SGLT2i users compared to diabetic subjects (P<0.05) (Figure 1 C). Instead, increased expressions of SGLT2 and NF-B(NF − κB) were observed in atherosclerotic plaques of patients with type 2 diabetes compared to nondiabetic and current SGLT2i users (Figure 1 D—F). Analysis of SGLT2 protein expression was also performed with additional antibodies from different manufacturers (Supplementary Figure 3 B—D,). Noteworthily, these pieces of evidence were strengthened by quantification of mRNA levels by RT-PCR showing that the *SLC5A2* gene, encoding SGLT2, was increased in plaques from diabetic patients who had never used SGLT2 inhibitors (never SGLTi users; $2^{-\Delta\Delta Ct} = 2.6 \pm 0.4$, $P < 0.01$ vs non-diabetic) compared to plaques from nondiabetic patients ($2^{-\Delta\Delta Ct} = 1.1 \pm 0.4$). Diabetic patients treated with SGLT2 inhibitors (SGLT2i users) showed a significant decrease in *SLC5A2* gene levels compared to never SGLTi users ($2^{-\Delta\Delta Ct} = 1.9 \pm 0.3$, $P < 0.05$ vs never SGLTi users) (Supplementary Figure 3 E).

The expression levels of SIRT6 and SGLT2 were associated with a more unstable plaque phenotype in patients with diabetes. Plaques from patients with diabetes had significantly more portions occupied by macrophages, nitrotyrosine, TNF-α, and MMP-9, along with a lesser collagen content compared to plaques from patients without diabetes (Figure 2). In contrast, the current SGLT2i users group presented a significantly smaller portion of plaque area occupied by

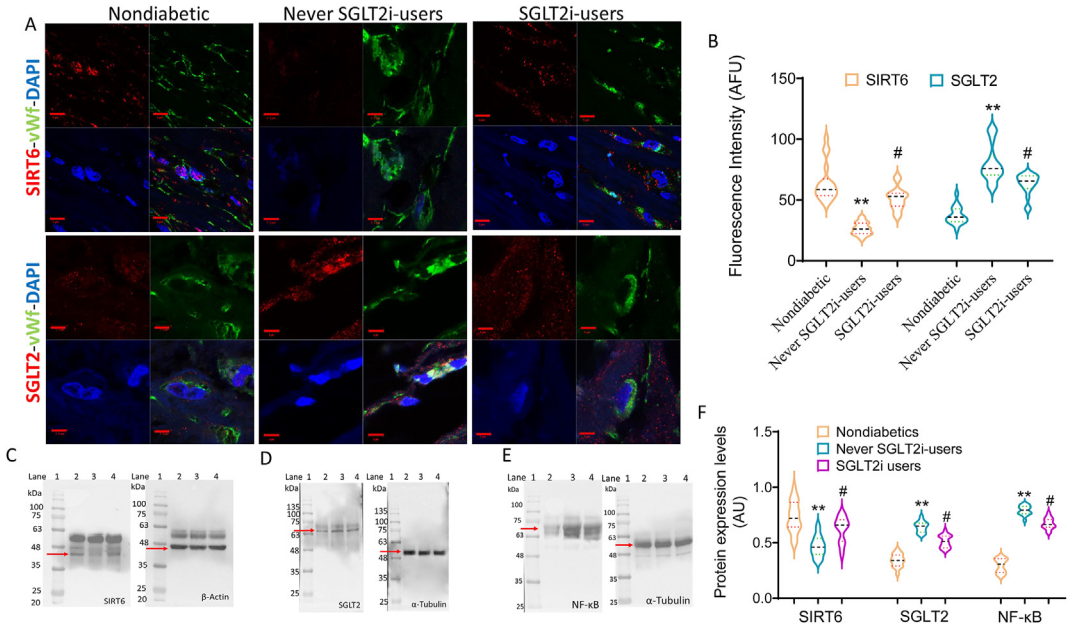

Figure 1: SIRT6 and SGLT2 expression in atherosclerotic plaques. (**A**) Representative confocal laser-scanning microscope images of SIRT6 and SGLT2 expression levels (red) in deparaffinized atherosclerotic plaques from non-diabetic patients, current SGLT2i users, and never SGLTi users. The von Willebrand factor (vWf, green) was used to properly localize the immunofluorescence signals in endothelial cells, while DAPI staining was used for nuclei counterstaining (blue). Scale Bar = 5 μm. (B) The ImageJ software carried out arbitrary fluorescence units (AFU) of SIRT6 and SGLT2. **p < 0.01 versus plaque specimen from patients without diabetes, #p < 0.05 never SGLT2i users. Protein expression levels of (C) SIRT6 (D) SGLT2 and (E) NF-B(NF − κB) in plaques from diabetic, non-diabetic, and diabetic SGLT2i-user patients. (F) Protein quantification was performed using β-Actin and α-tubulin as the internal control. SGLT2 protein expression detected by using anti-SGLT2 antibody from Cell Signaling Technology. Lane 1 = protein ladder molecular weight markers, lane 2 = non-diabetic, lane 3 = never SGLT2i users, lane 4 = SGLT2i users. The analysis of densitometric intensity was calculated with ImageJ software and expressed as arbitrary units (AU) with **p < 0.01 versus patients without diabetes, #p < 0.05 versus never SGLT2i users.

macrophages, nitrotyrosine, and MMP-9, along with more significant collagen content (Figure 2). The multivariate analyses showed that SGLT2 and SIRT6 plaque expressions were related to HbA1c levels (P = 0.008) and diabetic status (P = 0.001) independently from hypertension, dyslipidemia, heart disease, BMI, blood pressure, total cholesterol, HDL cholesterol, LDL cholesterol, and triglycerides. In the overall plaque studied (n = 523), inverse expression levels were observed between SGLT2, HbA1c, and SIRT6 (Supplementary Figure 2).

3.3. Clinical outcomes

After 2 years following endarterectomy, a multivariable Cox regression analysis, adjusted for age, hypertension, dyslipidemia, cigarette smoking, BMI, systolic blood pressure, total cholesterol, HDL and LDL cholesterol levels, triglycerides, beta-blockers calcium antagonist, and antiplatelet therapy, showed a significantly higher 2-year overall survival of MACE in patients without diabetes (Figure 3 A). Among patients with type 2 diabetes, the current SGLT2i users presented a significantly lower rate of MACE through 2 years compared to never SGLT2i users (P < 0.05) (Figure 3 B). MACE at the 2-year follow-up stratified by SGLT2 expression tertiles in the plaque of patients without and with type 2 diabetes was further assessed to translate molecular results into clinical endpoints. Cox multivariable regression analysis reported a lower survival from events among patients with higher SGLT2 plaque levels (Figure 3 C).

3.4. In vitro studies

SIRT6 and SGLT2 expression in endothelial cells under high-glucose conditions. To validate the observational data on atherosclerotic plaque sections from diabetic and non-diabetic patients, in vitro studies were performed to evaluate the effects of SGLT2i (canagliflozin) on the detrimental effect of high-glucose concentration on EC (TeloHAEC cell line), as well the relationship between the SIRT6 and SGLT2 pathway. First, SGLT2i was tested on the viability of the TeloHAEC cell line (Supplementary Figure 4). Dose—response experiments indicated that cell viability was not affected by treatment with SGLT2i from 0.25 μM to 10 μM for up to 8 h of treatment. According to previous studies [24], long-time exposure to SGLT2i resulted in cytotoxic and antiproliferative effects (Supplementary Figure 4). Treatment with SGLT2i during short-term exposure to high glucose showed significant effects starting at a concentration of 5 μM. Thus, the 5 μM concentration was used to test the in vitro effect of SGLT2i on SIRT6 protein levels and investigate the possible link between SGLT2 and SIRT6 during exposure to high glucose. Notably, SGLT2i (5 μM) counteracted the effects of high glucose by increasing the expression of SIRT6 (P < 0.05) (Figure 4 A-E). Moreover, short-time exposure to high glucose concentrations led to increased expression levels of SGLT2 (P < 0.01), which returned near to control levels in the presence of SGLT2i (P < 0.05) (Figure 4 A-E). The preincubation with SGLT1-blocking peptide (2 h at room temperature) before adding anti-SGLT2 primary antibody showed the absence of cross-reactivity between SGLT1 and SGLT2 antigens (Supplementary Figure 5 A, B). The same result was obtained using antibodies from different manufacturers (Cell Signaling Tecnology or Proteintech). Finally, SGLT2-siRNA experiments to transiently silence SGLT2 confirmed results observed in EC. (Supplementary Figure 5 C-E). Moreover, real-time PCR showed that SGLT2 mRNA levels were increased in EC cells exposed to high glucose ($2^{-\Delta\Delta Ct} = 1.6 \pm 0.2$, P < 0.01 vs control cells) compared to control cells ($2^{-\Delta\Delta Ct} = 0.8 \pm 0.3$). EC exposed to high glucose plus SGLT2i presented a reduction in SGLT2 levels compared to high glucose alone ($2^{-\Delta\Delta Ct} = 1.0 \pm 0.2$, P < 0.05 vs hGluc) (Supplementary Figure 5 F).

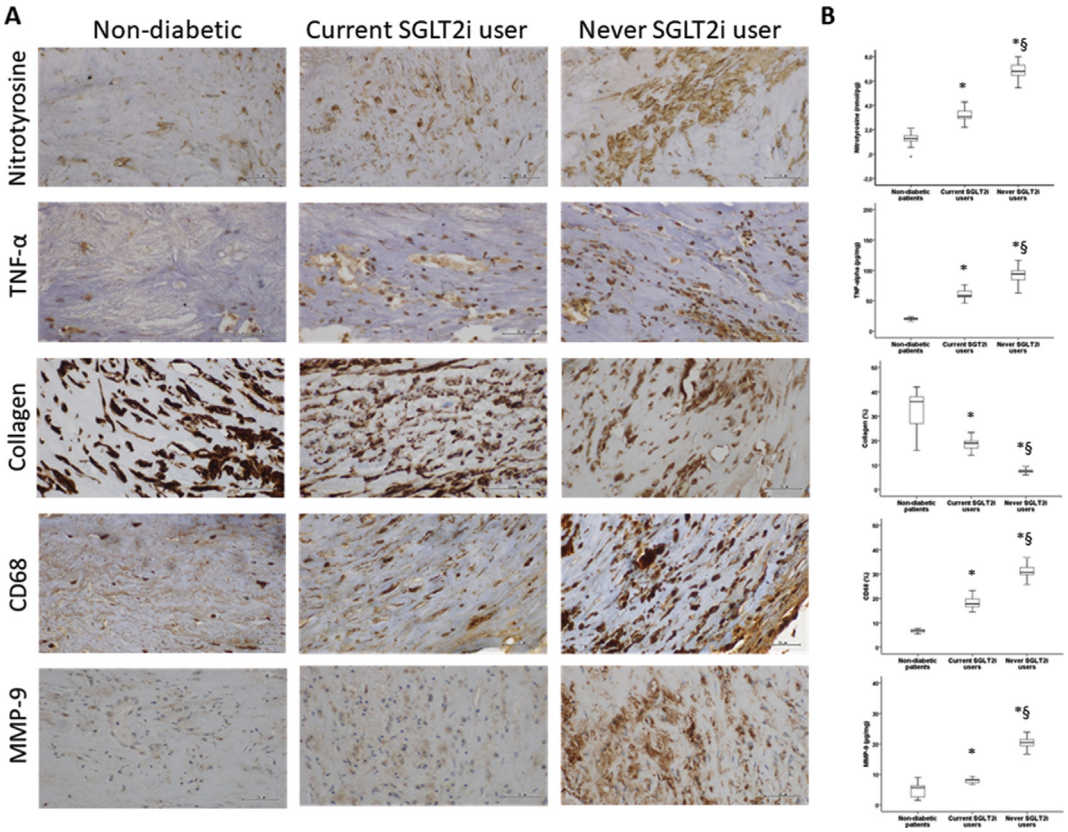

Figure 2: Atherosclerotic plaque phenotypes. (**A**) Immunochemistry for nitrotyrosine (X40), Tumor Necrosis Factor-alpha (TNF-α) (X40), collagen content (X40), macrophages (CD68) (X40), and Matrix metallopeptidase 9 (MMP-9) (X40), and in non-diabetic, current Sodium-Glucose co-transporter-2 inhibitor (SGLT2i)-user, and never SGLT2i-user asymptomatic plaques. Similar regions of plaque are shown. These results are typical of control, current SGLT2i-user, and never SGLT2i-user asymptomatic plaques. Negative controls were presented in Supplementary Figure 8. (B) Nitrotyrosine, TNF-α, collagen content, CD68, and MMP-9 in current SGLT2i-user and never SGLT2i-user asymptomatic plaques (The box plots show the median, 25th and 75th percentiles, range, and extreme values). *P $<$ 0.05 vs plaques from patients without diabetes. §P $<$ 0.05 vs current SGLT2i-user plaques.

EC that underwent high-glucose stimulation also showed increased levels of NF-B(NF $-$ κB) and MMP-9 proteins (P $<$ 0.01), which were partially reverted by SGLT2i (P $<$ 0.05) (Figure 4 F—H).

Effects of SGLT2i on endothelial oxidative stress and inflammation. In vitro experiments showed that SGLT2i displayed antioxidant and anti-inflammatory actions in EC exposed to high glucose. More specifically, results indicated that the mitochondrial ROS production observed in high glucose—treated cells (P $<$ 0.001) was inhibited by pre-treatment with SGLT2i (P $<$ 0.01 vs hGluc) (Figure 5 A-C). Treatment with Menadione (50 μM) confirmed the mitochondrial ROS localization (Supplementary Figure 6). Moreover, fluorimetric and cytometric analyses of extracellular and intracellular ROS showed similar results. In more detail, SGLT2i opposed the high glucose—induced intracellular ROS accumulation (637 $\pm$ 23.78 vs 970 $\pm$ 26.35 median fluorescence intensity (MFI) (P $<$ 0.01 vs hGluc) (Figure 5 D) and determined a consistent reduction (24%) of extracellular ROS content (P $<$ 0.05 vs hGluc) (Figure 5 E). The cytoprotective effect of SGLT2i was accompanied by a reduction of IL-6, IL-8, MCP-1, and TNF-α release during high-glucose treatment (Figure 5 F—I).

SIRT6 silencing blocks the beneficial effects of SGLT2i and acts as an SGLT2 upstream regulator. A transient SIRT6 gene silencing was performed to define the possible relationship between SIRT6 and SGLT2. Western blot analysis revealed that SGLT2i did not affect SIRT6 levels when gene silencing was performed (Figure 6 A-C). On the contrary, SIRT6 gene silencing determined an upregulation of SGLT2 expression (P $<$ 0.01) (Figure 6 B, C). Treatment with SGLT2i (5 μM) for 8 h in SIRT6-siRNA cells partially counteracted the increased levels of SGLT2 (P $<$ 0.05 vs SIRT6-siRNA). Interestingly, treatment of SIRT6 silenced cells with high glucose (SIRT6-siRNa+hGluc) determined a massive SGLT2 upregulation (P $<$ 0.05 vs SIRT6-siRNA and P $<$ 0.05 vs hGluc), with SGLT2i unable to revert this effect (Figure 6 D-E). Likewise, the increased levels of TNF-α in the cell exposed to high glucose, SIRT6-siRNA, and even more to SIRT6-siRNA+hGluc (P $<$ 0.05 vs SIRT6siRNAa and P $<$ 0.05 s hGluc) were not affected by SGLT2i (Figure 6 F—H). These findings suggest that SIRT6 mediates the beneficial effects of SGLT2i. These observations were also supported by cytotoxicity and proinflammatory cytokine evaluation (Figure 7 A-C). Indeed, the pre-treatment with SGLT2i (5 μM) did not restore the cytotoxicity induced by SIRT6-siRNA (P $<$ 0.01) and the release of IL-8 and IL-6 (P $<$ 0.001) occurring under high-glucose conditions. Finally, the pleiotropic effects of SGLT2i mediated by SIRT6 were underlined by ROS measurement (Figure 7 D-G and Supplementary Figure 7 A). In SIRT6-silenced cells, SGLT2i was ineffective in counteracting mitochondrial and intracellular accumulation of ROS (Figure 7 D-G) and failed to restore NF-κB protein

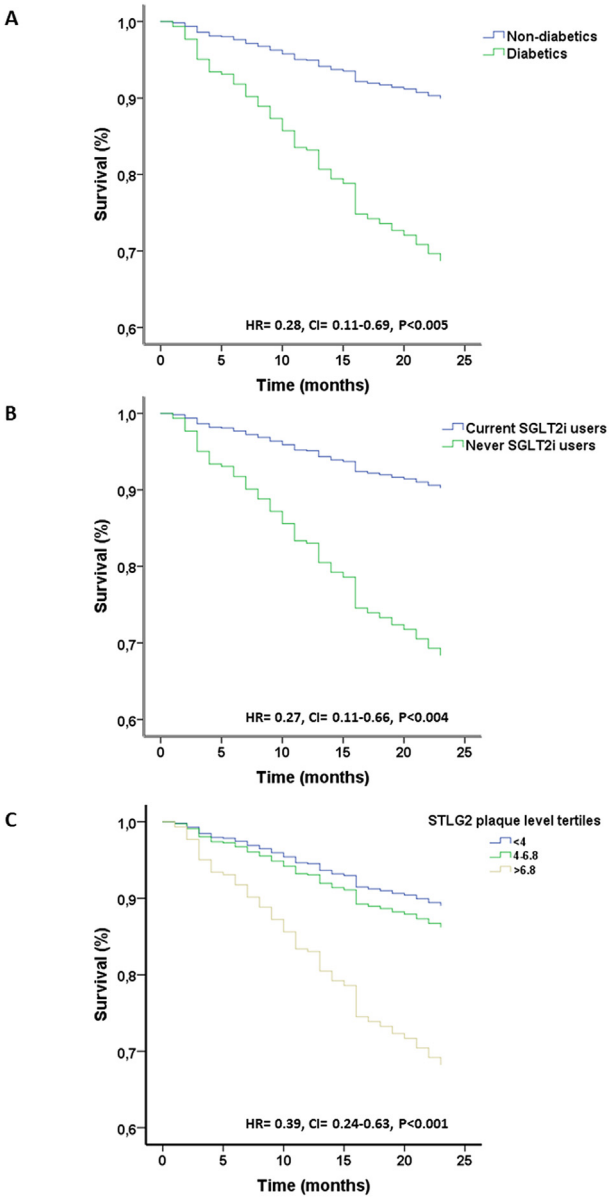

Figure 3: Survival from MACE Cox regression analysis (adjusted for age, sex, BMI, blood pressure, heart rate, cholesterol, HDL cholesterol, LDL cholesterol, triglyceride levels, heart disease, hypertension, dyslipidemia, smoking, b-blockers, ACE inhibitors, calcium inhibitors, thiazide diuretics, and aspirin) according to diabetic status (A), SGLT2i therapy (B), and SGLT2 carotid atherosclerotic plaque content (C).

expression (Figure 7 H, I and Supplementary Figure 7 B, C). Of note, the transient SGLT2 gene silencing did not modulate the SIRT6 expression levels, thus suggesting a role of SIRT6 as an upstream regulator of SGLT2 signaling in TeloHAEC (Figure 7 J, K). Taken together, results provided novel insight into the beneficial effects of SGLT2i in endothelial cells under metabolic stress induced by hyperglycemia and provided the first in vitro evidence of SIRT6 involvement.

4. DISCUSSION

Here, we report that endothelial cells of human carotid atherosclerotic plaques express SGLT2 protein for the first time. Moreover, we provide novel insights into the relationship between SGLT2 and SIRT6 in the inflammatory process of atherosclerotic plaques of patients with type 2 diabetes. Specifically, endothelial expression of SGLT2 was upregulated in diabetic atherosclerotic lesions compared with nondiabetic lesions. The increased expression of SGLT2 was associated with higher oxidative stress, NF-B(NF $-$ κB), proinflammatory cytokines, and MMP-9 levels, along with lower SIRT6 expression and interstitial collagen content. As a whole, these factors might increase the risk of future acute ischemic events precipitated by inflammatory-dependent rupture of atherosclerotic plaques. We provide evidence that in patients with type 2 diabetes, the drugs that work on the SGLT2 system, such as SGLT2i, may prevent progression to an unstable plaque phenotype and the upregulation of SGLT2 endothelial expression.

Previous studies evaluated the mechanisms whereby hyperglycemia-induced oxidative stress compromises vascular endothelial function. They also provide background for a recently published study illustrating the beneficial impacts of endothelial SGLT2i in attenuating hyperglycemia-induced vascular dysfunction in vitro and/or in experimental animal models [25–27]. However, many concerns arise from extending the findings of these studies from mice to humans, pointing to the need to validate the work using vascular tissues from humans. To date, there is no evidence about the possible role of endothelial SGLT2 protein in the specific pathway(s) transducing diabetic milieu stimuli in the modulation of the atherosclerotic plaque phenotype toward instability and vascular events. The novelty of this study is represented by the evidence that the endothelial expression of SGLT2 is more markedly upregulated in the asymptomatic plaques from patients with diabetes than asymptomatic plaques from patients without diabetes and is associated with more macrophages and TNF-α levels. These results suggest that the presence of an active inflammatory reaction in plaques from patients with diabetes may be associated with a higher expression of SGLT2 in endothelial cells. In line with such evidence, higher expression of SGLT2 and concomitantly higher levels of oxidative stress (nitrotyrosine levels), MMP-9 levels, and thinning of the fibrous cap, as evidenced by reduced plaque collagen content, were found in plaques obtained from the asymptomatic patients with type 2 diabetes compared with patients without diabetes. In agreement with the difference in SGLT2 expression patterns, the histological milieu of the lesions appears different in cellularity but not in the degree of vessel stenosis, thus suggesting that diabetic and nondiabetic lesions are only different regarding SGLT2 protein expression and inflammatory burden. Therefore, in this study, the observed increased expression of SGLT2 in carotid plaques of patients with type 2 diabetes might be associated with the expansion of oxidative and inflammatory processes, thinning of the fibrous cap, and plaque instability. As background for this association, we hypothesize that endothelial SGLT2 protein may increase atherosclerotic plaque's inflammatory burden through endothelial SIRT6 reduction. Accordingly, our data evidence a higher expression of SGLT2 and, concomitantly, a lower SIRT6 expression in endothelial cells from diabetic atherosclerotic plaque than non-diabetic atherosclerotic plaque.

Quantitative experiments of SGLT2 mRNA expression in human endothelial cells demonstrated that exposure to high glucose also resulted in the appearance of SGLT2 mRNA levels as assessed following mRNA purification after 1-hour and 4-hour treatment periods. These effects were associated with a significantly increased SGLT2 protein level [28]. These data support our results, showing that the SLC5A2 gene was increased in plaques from diabetic patients never using SGLT2 inhibitors compared to plaques from nondiabetic patients. On the contrary, diabetic patients treated with SGLT2 inhibitors showed a significant

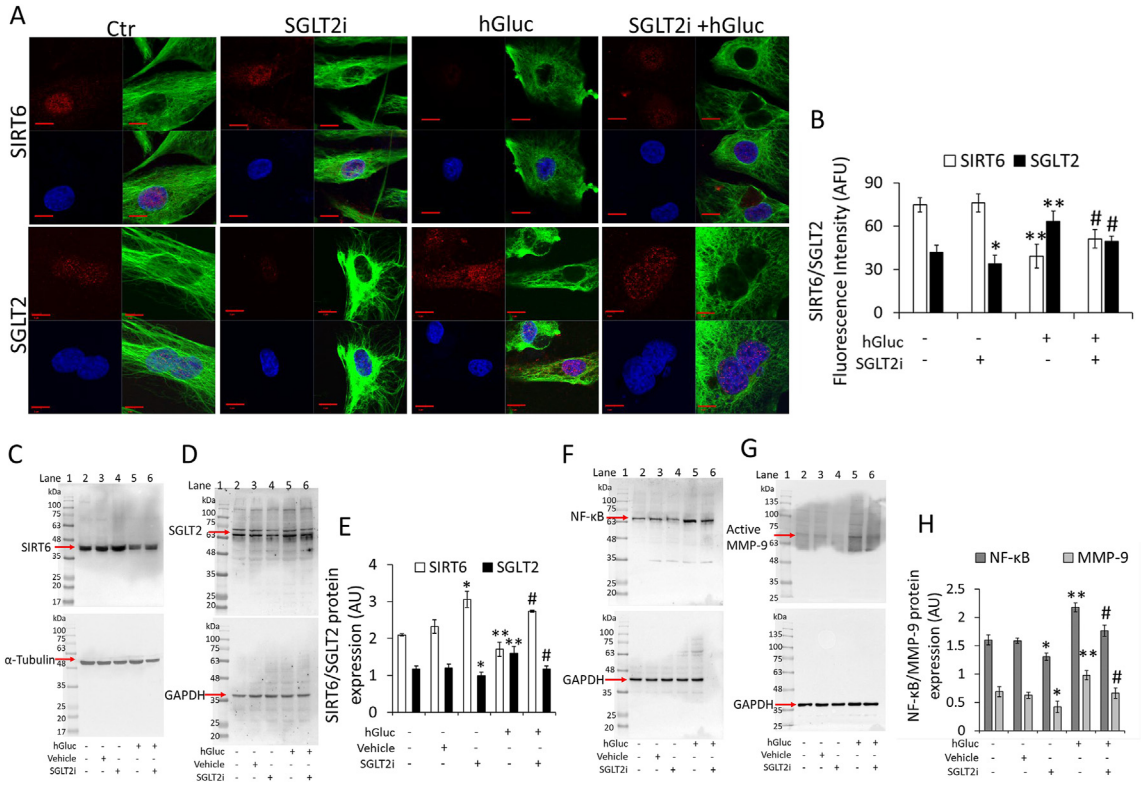

Figure 4: SGLT2 inhibitor restored SIRT6 expression levels during hyperglycemia. (A, B) Representative confocal images of SIRT6 and SGLT2 (red), vimentin (green), and (G) their fluorescence intensity determination, performed by using ImageJ software and expressed as arbitrary fluorescence units. Scale Bar = 10 μm *p < 0.05 vs Ctr, **p < 0.01 vs Ctr, #p < 0.05 vs hGluc. (C–E) Representative Western blot images and analysis of SIRT6 and SGLT2 expression levels in endothelial cells pre-treated for 8 h with 5 μM SGLT2i before 48 h hGluc (25 mM) stress induction. Lane 1 = protein ladder molecular weight markers, lane 2 = Ctr, lane 3 = vehicle, lane 4 = SGLT2i, lane 5 = hGluc, lane 6 = SGLT2i+hGluc. (F–H) Western blot image and analysis of NF-kB and MMP-9 expression level in EC pre-treated for 8 h with 5 μM SGLT2i before 48 h hGluc (25 mM) stress induction. Lane 1 = protein ladder molecular weight markers, lane 2 = Ctr, lane 3 = vehicle, lane 4 = SGLT2i, lane 5 = hGluc, lane 6 = SGLT2i+hGluc. The analysis of densitometric intensity was calculated with ImageJ software and expressed as arbitrary units. α-Tubulin or GAPDH were used as internal control. *p < 0.05 vs Ctr, **p < 0.01 vs Ctr, #p < 0.05 vs hGluc.

decrease in SLC5A2 gene levels compared to never SGLTi users. In agreement with ex vivo experiments, SGLT2 mRNA was also increased in EC cells exposed to high glucose compared to control cells. The addition of SGLT2i before short-term exposure to high glucose determined a reduction in SGLT2 levels compared to hGluc alone. Thus, we speculate that the impaired SGLT2/SIRT6 pathway plays a central role in the atherosclerotic plaque progression toward instability. This hypothesis is supported by the in vitro study in cultured endothelial cells, which demonstrates that high glucose increases SGLT2 expression and inflammatory mediators and reduces SIRT6 expression.

These data are consistent with our previous findings: that endothelial loss of SIRT6 was paralleled by increased expression of the proinflammatory NF-B(NF − κB) and, conversely, that overexpression of SIRT6 is associated with a downregulation of NF-B(NF − κB) activity as well as the expression of its target genes [14]. Our data collectively suggest that the endothelial SGLT2/SIRT6 pathway modulates vascular oxidative stress and inflammation in diabetic atherosclerotic plaques. In this context, previous reports evidenced the involvement of SGLT2 in the regulation of sirtuins, particularly under conditions of metabolic diseases such as diabetes and high-fat diet–induced obese mice [9]. In experimental models of diabetes and obesity, SGLT2/SIRT6 deregulation plays a pivotal role in the pathogenesis of heart dysfunction [10], liver steatosis, renal disease, and renal tubule diseases [29,9]. Moreover, SGLT2i therapy may exert a protective effect in the same experimental models by reducing SGLT2 protein and increasing SIRT1. However, no evidence exists regarding the potential role of SGLT2i in regulating the SGLT2/SIRT6 pathway in the atherosclerotic plaques of patients with diabetes. In this study, we observed that SIRT6 expression in atherosclerotic plaques was inversely correlated with SGLT2 levels. SIRT6 antagonizes NF-B(NF − κB)–induced gene expression programs by associating with chromatin-bound NF-B(NF − κB), directing deacetylation of histone H3 lysine 9 (H3K9] and destabilizing binding of NF-B(NF − κB) to chromatin [30]. Thus, we hypothesized that the decreased expression of SIRT6 in plaques, as a consequence of SGLT2 increase, may enhance NF-B(NF − κB) activity, representing a crucial step in the pathophysiology of plaques from patients with diabetes instability. In this context, our data suggest the possibility of a novel pathway through which the SGLT2 impairment, by reducing SIRT6 expression, could affect the inflammatory burden in diabetic atherosclerotic plaques. Thus, modulation of SIRT6 through SGLT2i could benefit many inflammatory diseases associated with endothelial dysfunction [31] and play a pivotal role in stabilizing diabetic atherosclerotic plaques. In this context, the present findings show a stimulatory effect of the drugs that work on the SGLT2 system, including SGLT2i, on the SIRT6 pathway in diabetic lesions. Indeed, at the same blood glucose level, diabetic patients treated with SGLT2i had the lowest endothelial SGLT2 expression, inflammatory plaque cells, cytokines, oxidative stress, and MMP-9, associated with the

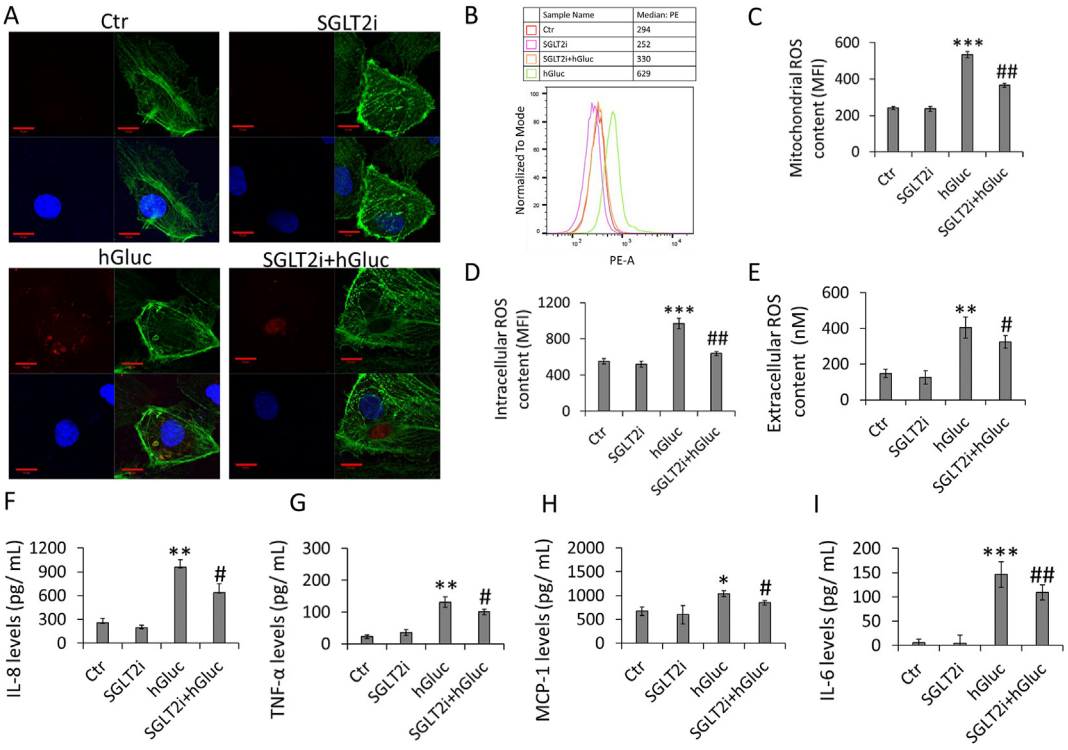

Figure 5: SGLT2i counteracted the high glucose–induced oxidative stress. (A) Representative images of confocal laser scanning analyses of mitochondrial ROS generation detected by MitoSOX probe and (B) mitochondrial superoxide levels assessed by flow cytometry analysis. (C) Results are expressed as median fluorescence intensity (MFI). Scale bars = 10 μm. Cytoskeleton is marked with Phalloidin 488 (green) while DAPI was used in nuclei counterstaining (blue). (D) Intracellular and (E) extracellular ROS content detected, respectively, by DCF probe and Amplex Red kit. Endothelial cells were pre-treated (8 h) or not pre-treated with SGLT2i 5 μM before 48 h of high glucose (25 mM) treatment. $^{**}p < 0.01$ vs Ctr, $^{***}p < 0.001$ vs Ctr, $\#p < 0.05$ vs hGluc, $\#\#p < 0.01$ vs hGluc. (F–I) Cytokine levels in EC measured after pre-treatment (8 h) or no pre-treatment with SGLT2i 5 μM before 48 h of high glucose (25 mM) induction. $^{*}p < 0.05$ vs Ctr. $^{**}p < 0.01$ vs Ctr, $^{***}p < 0.001$ vs Ctr, $\#p < 0.05$ vs hGluc, $\#\#p < 0.01$ vs hGluc.

highest SIRT6 expression and content of plaque interstitial collagen. Thus, patients assigned to SGLT2i-based therapy had less progression to an unstable plaque phenotype than those treated without incretin-based therapy. In particular, the increased SIRT6 expression observed in plaques from diabetic patients among the current SGLT2i users suggests a low inflammatory activity linked to decreased NF-B(NF − κB) activation. This hypothesis is supported by the results of in vitro experiments on human aorta endothelial cells, showing that the increased expression of NF-B(NF − κB) parallels the loss of SIRT6 during short-term exposure to high glucose.

In contrast, overexpression of SIRT6 upon pre-treatment with SGLT2i relates to a decreased NF-B(NF − κB) expression. In vascular inflammation, endothelial progenitor cells (EPCs) and activated EC are critically involved in the formation of new blood vessels, which play an important role in several pathologies, including atherosclerosis and diabetes [32]. A strong correlation between the number of circulating EPCs and the combined Framingham risk factor score for atherosclerosis exists, suggesting that EPCs can be used as a predictive biomarker for cardiovascular risk and vascular function [33]. Our data, according to reports showing that the loss of SIRT6 in EC is associated with increased expression of the cell adhesion molecule ICAM-1, NF-B(NF − κB), and senescence [34], shed light on the role of SIRT6 as a regulator of endothelial function during altered glucose homeostasis within a pathway that links inflammation, metabolic diseases, and atherosclerosis. The evidence that SGLT2 transient gene silencing could not modulate SIRT6 expression levels suggests that SIRT6 is the upstream SGLT2 modulator.

As a whole, our data may have substantial clinical implications, as in an extensive series of carotid endarterectomy specimens, it has been shown that plaque inflammation is a significant determinant of ischemic events in patients affected by the atherosclerotic carotid disease [35]. Whether SGLT2i reduces clinical events in patients with carotid plaque requires further data from controlled clinical trials. However, our observational data suggest that SGLT2i therapy reduces the risk of clinical events in atherosclerotic patients with type 2 diabetes with the same glycemic control from propensity score-matched patients. Therefore, the direct anti-inflammatory effects of SGLT2i, which decrease endothelial SGLT2 expression and go above and beyond glycemic control, should also be considered. However, data from a metanalysis study observed that SGLT2i are neutral in all aspects of CV outcomes [36].

On the other hand, as also reported by the authors, the metanalysis presents substantial limitations. The selection criteria were extremely restrictive and could have excluded numerous observational and randomized trials. Although clinical trials are considered the ''gold standard'' method of testing a hypothesis, large population-based observational studies can give important information about the real-life applications of the drug in question. The main limitations to generalizing the metanalysis data were the differences in the baseline, inclusion criteria, and definitions of endpoints in all analyzed studies.

In conclusion, we demonstrated that SGLT2i reduced plaque macrophage infiltration and MMP-9 expression, resulting in an increased plaque collagen content and a thickened fibrous cap in plaques from human patients with diabetes. As these plaque characteristics are

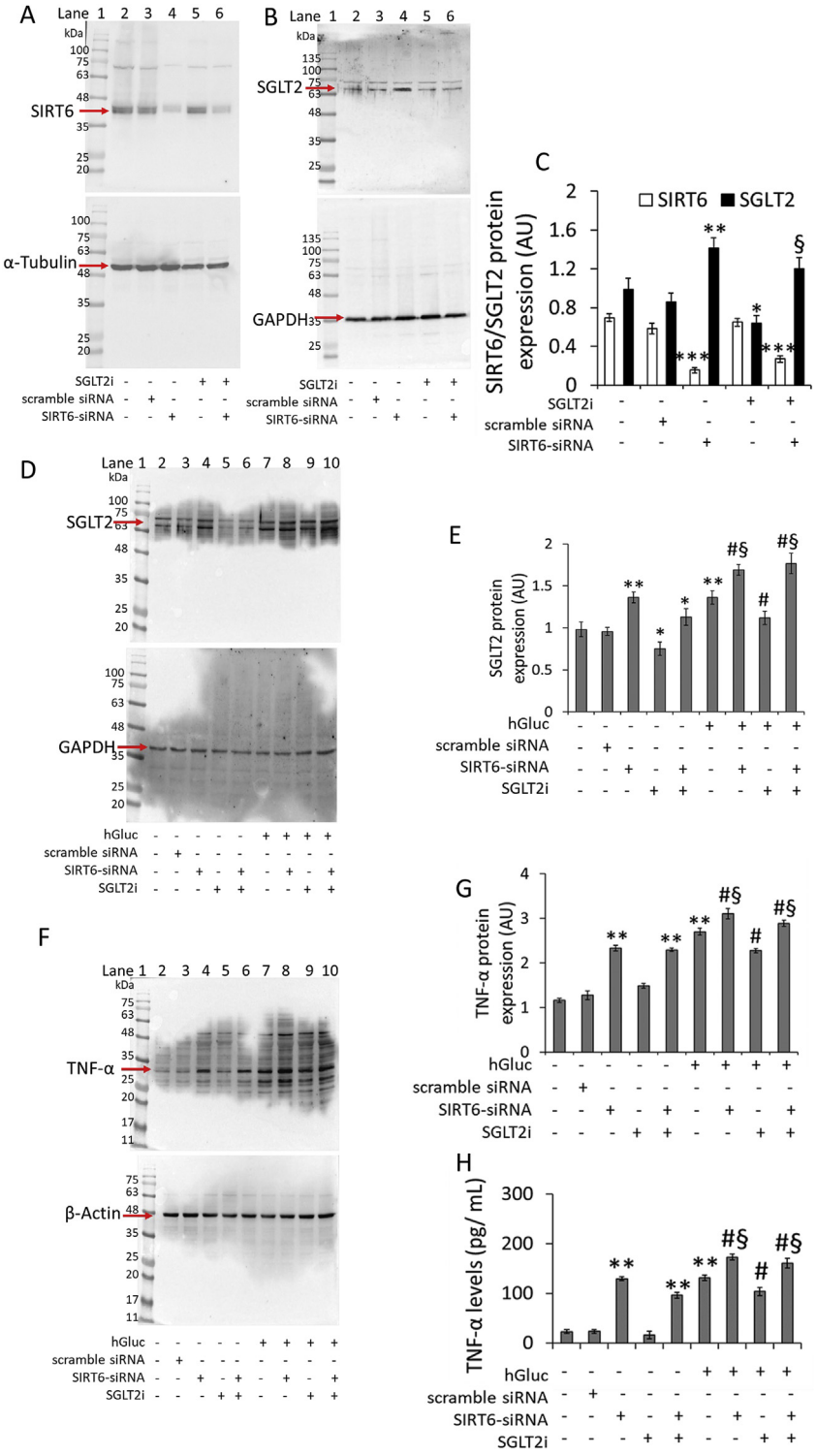

Figure 6: SIRT6 mediates both SGLT2 expression and endothelial response against hyperglycemia damages. (A) SIRT6 and (B) SGLT2 expression levels in EC after SIRT6 silencing and/or SGLT2i pre-treatment for 8 h. Lane 1 = protein ladder molecular weight markers, lane 2 = Ctr, lane 3 = scramble siRNA, lane 4 = SIRT6-siRNA, lane 5 = SGLT2i, lane 6 = SIRT6-siRNA+SGLT2i. α-Tubulin or GAPDH were used as internal control. (C) The analysis of densitometric intensity was calculated with ImageJ software and expressed as arbitrary units. *$p < 0.05$ vs Ctr, **$p < 0.01$ vs Ctr, ***$p < 0.001$ vs Ctr, §$p < 0.05$ vs SIRT6-siRNA. (D, E) SGLT2 and (F, G) TNF-α protein levels assessed by Western blot analyses. Endothelial cells, after SIRT6 silencing, were subjected or not subjected to 8 h of pre-treatment with SGLT2i before starting 48 h of hGluc stress induction. Lane 1 = protein ladder molecular weight markers, lane 2 = Ctr, lane 3 = scramble siRNA, lane 4 = SIRT6-siRNA, lane 5 = SGLT2i, lane 6 = SIRT6-siRNA+SGLT2i, lane 7 = hGluc, lane 8 = SIRT6-siRNA+hGluc, lane 9 = SGLT2i+hGluc, lane 10 = SIRT6 siRNA+SGLT2i+hGluc. β-Actin or GAPDH were used as the internal control. (H) TNF-α cytokine levels in EC measured after SIRT6 silencing and SGLT2i pre-treatment before starting 48 h of hGluc incubation. *$p < 0.05$ vs Ctr, **$p < 0.01$ vs Ctr, #$p < 0.05$ vs hGluc, §$p < 0.05$ vs SIRT6 siRNA.

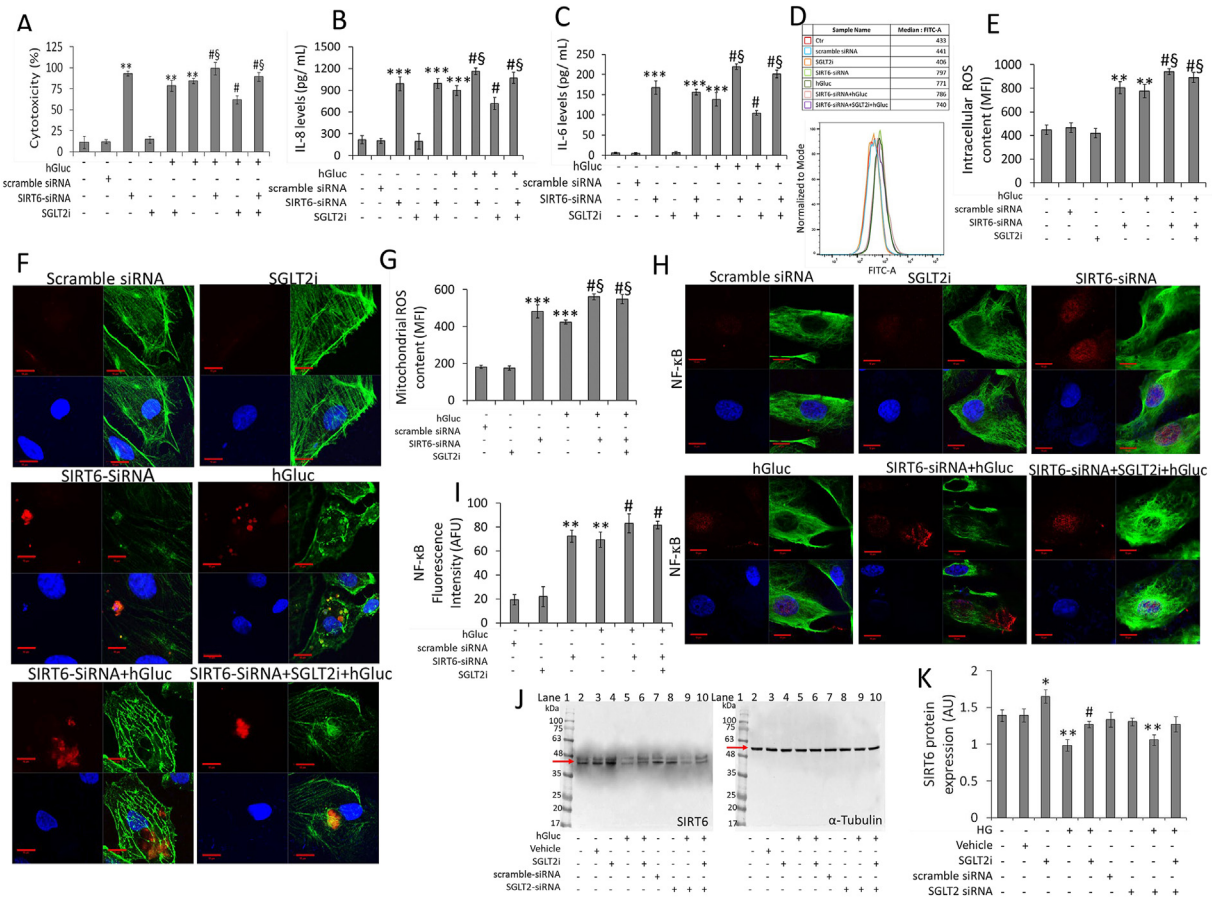

Figure 7: SIRT6 gene silencing blocks the SGLT2i protective effects against hyperglycemia injury. (A) Cytotoxicity, assessed by LDH Assay Kit-WST, and (B, C) cytokine levels in endothelial cells measured after SIRT6 silencing and hGluc stress condition for 48 h, preceded or not by SGLT2i pre-treatment for 8 h. (D, E) Intracellular ROS content detected by flow cytometry analysis using DCF probe. EC after SIRT6-siRNA were subjected or not subjected to 8 h SGLT2i pre-treatment before starting 48 h of incubation with hGluc. (F) Representative images of confocal laser scanning analyses of mitochondrial ROS generation detected by MitoSOX probe and (G) mitochondrial superoxide levels detected by flow cytometry analysis. Results are expressed as median fluorescence intensity (MFI). Scale bars = 10 μm. The cytoskeleton is marked with Phalloidin 488 (green), while DAPI was used for the nuclei counterstain (blue). (H) Representative confocal images of NF-B(NF − κB) (red) and vimentin (green) and (I) fluorescence intensity analysis, performed using ImageJ software, expressed as arbitrary fluorescence units. (J, K) SIRT6 protein levels, assessed by Western blot analysis. Endothelial cells, after SGLT2 silencing, were subjected or not subjected to 8 h of pre-treatment with SGLT2i before starting 48 h of hGluc stress induction. Lane 1 = protein ladder molecular weight markers, lane 2 = Ctr, lane 3 = vehicle, lane 4 = SGLT2i, lane 5 = hGluc, lane 6 = SGLT2i+hGluc, lane 7 = scramble siRNA, lane 8 = SGLT2-siRNA, lane 9 = SGLT2-siRNA+hGluc, lane 10 = SGLT2-siRNA+SGLT2i+hGluc. The analysis of densitometric intensity was calculated with ImageJ software and expressed as arbitrary units (AU). α-Tubulin was used as an internal control. *p < 0.05 vs Ctr, **p < 0.01 vs Ctr, #p < 0.05 vs hGluc.

features of plaque stability, the results of this study suggest that SGLT2i reduces plaque vulnerability. These findings may be of clinical importance for patients with type 2 diabetes mellitus, who are known to exhibit a higher burden of inflamed, rupture-prone atherosclerotic plaques in comparison to non-diabetic subjects [37]. Future studies are needed to determine whether the beneficial effects of SGLT2i on features of plaque vulnerability through the SIRT6 pathway translate into a reduction of cardiovascular events in patients with type-2 diabetes treated with SGLT2i-based regimes.

AUTHOR CONTRIBUTIONS

Conception, design and interpretation of data: Raffaele Marfella, Nunzia D'Onofrio, Celestino Sardu, Maria Luisa Balestrieri, and Giuseppe Paolisso.
Acquisition of data: Lucia Scisciola, Fabrizio Turriziani, Lella Petrella, Mara Fanelli, Ciro Mauro, Fabio Minicucci, and Fulvio Furbatto.
Analysis of data: Maria Luisa Balestrieri, Nunzia D'Onofrio, Ferdinando Carlo Sasso Franca Ferraraccio, and Iacopo Panarese.
Manuscript revision: Piero Modugno, Massimo Massetti, Michelangela Barbieri, Massimo Federici, Giuseppe Paolisso, Maria Luisa Balestrieri, and Raffaele Marfella.
The guarantor is Raffaele Marfella

FUNDING

PRIN: PROGETTI DI RICERCA DI RILEVANTE INTERESSE NAZIONALE — Bando 2017 Prot. 2017FM74HK.

ACKNOWLEDGMENTS

The authors are grateful to Dr. Luigi Ruggiero (Geriatric Unit of Università degli Studi della Campania "Luigi Vanvitelli") for important work in the clinical evaluation of patients admitted at our department, as well as to Dr. Giovanna Ferrara (Pathological

Anatomy section of Università degli Studi della Campania "Luigi Vanvitelli") for important technical support.

CONFLICT OF INTEREST

The authors have declared that no conflict of interest exists.

APPENDIX A. SUPPLEMENTARY DATA

Supplementary data to this article can be found online at https://doi.org/10.1016/j.molmet.2021.101337.

REFERENCES

[1] Einarson, T.R., Acs, A., Ludwig, C., Panton, U.H., 2018. Prevalence of cardiovascular disease in type 2 diabetes: a systematic literature review of scientific evidence from across the world in 2007-2017. Cardiovascular Diabetology 17(1):83.

[2] Sugiyama, T., Yamamoto, E., Bryniarski, K., Xing, L., Fracassi, F., Lee, H., et al., 2018. Coronary plaque characteristics in patients with diabetes mellitus who presented with acute coronary syndromes. J Am Heart Assoc 7:e009245.

[3] Paolisso, P., Foà, A., Bergamaschi, L., Donati, F., Fabrizio, M., Chiti, C., et al., 2021. Hyperglycemia, inflammatory response and infarct size in obstructive acute myocardial infarction and MINOCA. Cardiovascular Diabetology 20:33.

[4] Kanai, Y., Lee, W.S., You, G., Brown, D., Hediger, M.A., 1994. The human kidney low affinity Na+/glucose cotransporter SGLT2. Delineation of the major renal reabsorptive mechanism for D-glucose. Journal of Clinical Investigation 93:397—404.

[5] Gallo, L.A., Wright, E.M., Vallon, V., 2015. Probing SGLT2 as a therapeutic target for diabetes: basic physiology and consequences. Diabetes and Vascular Disease Research 12:78—89.

[6] Ferrannini, G., Cosentino, F., 2021. SGLT2i: new perspectives in diabetes and kidney disease. Eur Heart J Cardiovasc Pharmacother Jan 25 pvab003.

[7] Ni, L., Yuan, C., Chen, G., Zhang, C., Wu, X., 2020. SGLT2i: beyond the glucose-lowering effect. Cardiovascular Diabetology 19:98.

[8] El-Daly, M., Pulakazhi, V.V., Saifeddine, M., Mihara, K., Kang, Fedak, S.P., et al., 2018. Hollenberg, Hyperglycaemic impairment of PAR2-mediated vasodilation: prevention by inhibition of aortic endothelial sodium-glucose-co-Transporter-2 and minimizing oxidative stress, Vasc. Pharmacol 109: 56—71.

[9] Umino, H., Hasegawa, K., Minakuchi, H., Muraoka, H., Kawaguchi, T., Kanda, T., et al., 2018. High basolateral glucose increases sodium-glucose cotransporter 2 and reduces sirtuin-1 in renal tubules through glucose transporter-2 detection. Scientific Reports 8:6791.

[10] Packer, M., 2020. Cardioprotective effects of Sirtuin-1 and its downstream effectors: potential role in mediating the heart failure benefits of SGLT2 (Sodium-Glucose Cotransporter 2) inhibitors. Circ Heart Fail 13:e007197.

[11] Khemais-Benkhiat, S., Belcastrom, E., Idris-Khodja, N., Park, S.H., Amoura, L., Abbas, M., et al., 2020. Angiotensin II-induced redox-sensitive SGLT1 and 2 expression promotes high glucose-induced endothelial cell senescence. Journal of Cellular and Molecular Medicine 24:2109—2122.

[12] Terasaki, M., Hiromura, M., Mori, Y., Kohashi, K., Nagashima, M., Kushima, H.T., et al., 2015. Hirano, Amelioration of hyperglycemia with a sodium-glucose cotransporter 2 inhibitor prevents macrophage-driven atherosclerosis through macrophage foam cell formation suppression in type 1 and type 2 diabetic mice. PloS One 10:e143396.

[13] Leng, W., Ouyang, X., Lei, X., Wu, M., Chen, L., Wu, Q., et al., 2016. The SGLT-2 inhibitor Dapagliflozin has a therapeutic effect on atherosclerosis in diabetic ApoE−/− mice. Mediators of Inflammation, 1—13.

[14] Balestrieri, M.L., Rizzo, M.R., Barbieri, M., Paolisso, P., D'Onofrio, N., Giovane, A., et al., 2015. Sirtuin 6 expression and inflammatory activity in diabetic atherosclerotic plaques: effects of incretin treatment. Diabetes 64: 1395—1406.

[15] Young, B., Moore, W.S., Robertson, J.T., Toole, J.F., Ernst, C.B., Cohen, S.N., et al., 1996. An analysis of perioperative surgical mortality and morbility in the Asymptomatic Carotid Atherosclerosis Study. Stroke 27:2216—2224.

[16] ADA, 2020. Classification and diagnosis of diabetes: standards of medical care in diabetes. Diabetes Care vol. 43(Supplement 1):S14—S31.

[17] Mansueto, G., Costa, D., Capasso, E., Varavallo, F., Brunitto, G., Caserta, R., et al., 2019. The dating of thrombus organization in cases of pulmonary embolism: an autopsy study. BMC Cardiovascular Disorders 19(1):250.

[18] Sadile, F., Bernasconi, A., Carbone, F., Lintz, F., Mansueto, G., 2017. Histological fibrosis may predict the failure of core decompression in the treatment of osteonecrosis of the femoral head. International Journal of Surgery 44:303—308.

[19] Marfella, R., D'Amico, M., Di Filippo, C., Baldi, A., Siniscalchi, M., Sasso, F.C., et al., 2006. Increased activity of the ubiquitin-proteasome system in patients with symptomatic carotid disease is associated with enhanced inflammation and may destabilize the atherosclerotic plaque: effects of rosiglitazone treatment. Journal of the American College of Cardiology 47:2444—2455.

[20] D'Onofrio, N., Sardu, C., Paolisso, P., Minicucci, F., Gragnano, F., Ferraraccio, F., et al., 2020. MicroRNA-33 and SIRT1 influence the coronary thrombus burden in hyperglycemic STEMI patients. Journal of Cellular Physiology 235(2):1438—1452.

[21] Balestrieri, M.L., Servillo, L., Esposito, A., D'Onofrio, N., Giovane, A., Casale, R., et al., 2013. Poor glycaemic control in type 2 diabetes patients reduces endothelial progenitor cell number by influencing SIRT1 signalling via platelet-activating factor receptor activation Diabetologia 56(1):162—172.

[22] Endarterectomy for asymptomatic carotid artery stenosis: executive committee for the asymptomatic carotid atherosclerosis study. Journal of the American Medical Association 23, 1995:1421—1428.

[23] Keyhani, S., Cheng, E.M., Hoggatt, K.J., Austin, P.C., Madden, E., Hebert, P.L., et al., 2020. Comparative effectiveness of carotid endarterectomy vs initial medical therapy in patients with asymptomatic carotid stenosis. JAMA Neurol 77:1110—1121.

[24] Behnammanesh, G., Durante, Z.E., Peyton, K.J., Martinez-Lemus, L.A., Brown, S.M., Bender, S.B., et al., 2019. Canagliflozin inhibits human endothelial cell proliferation and tube formation. Frontiers in Pharmacology 10:362.

[25] Pulakazhi Venu, V.K., El-Daly, M., Saifeddine, M., Hirota, S.A., Ding, H., Triggle, C.R., et al., 2019. Minimizing hyperglycemia-induced vascular endothelial dysfunction by inhibiting endothelial sodium-glucose cotransporter 2 and attenuating oxidative stress: implications for treating individuals with type 2 diabetes. Canadian Journal of Diabetes 43:510—514.

[26] Ganbaatar, B., Fukuda, D., Shinohara, M., Yagi, S., Kusunose, K., Yamada, H., et al., 2020. Empagliflozin ameliorates endothelial dysfunction and suppresses atherogenesis in diabetic apolipoprotein E-deficient mice. European Journal of Pharmacology 15:875. https://doi.org/10.1016/j.ejphar..173040.

[27] Han, J.H., Oh, T.J., Lee, G., Maeng, H.J., Lee, D.H., Kim, K.M., et al., 2017. The beneficial effects of empagliflozin, an SGLT2 inhibitor, on atherosclerosis in ApoE (-/-) mice fed a western diet. Diabetologia 60:364—376. https://doi.org/10.1007/s00125-016-4158-2.

[28] Benkhiat, S.K., Belcastro, E., Khodja, N.I., Park, S.H., Amoura, L., Abbas, M., et al., 2020. Angiotensin II-induced redox-sensitive SGLT1 and 2 expression promotes high glucose-induced endothelial cell senescence. Journal of Cellular and Molecular Medicine 24(3):2109—2122. https://doi.org/10.1111/jcmm.14233.

[29] Suga, T., Sato, K., Ohyama, T., Matsui, S., Kobayashi, T., Tojima, H., et al., 2020. Ipragliflozin-induced improvement of liver steatosis in obese mice may involve sirtuin signaling. World Journal of Hepatology 12:350—362.

[30] Beauharnois, J.M., Bolívar, B.E., Welch, J.T., 2013. Sirtuin 6: a review of biological effects and potential therapeutic properties. Molecular BioSystems 9:1789–1806.

[31] Sundaresan, N.R., Vasudevan, P., Zhong, L., Kim, G., Samant, S., Parekh, V., et al., 2012. The sirtuin SIRT6 blocks IGF-Akt signaling and development of cardiac hypertrophy by targeting c-Jun. Natura Med 18:1643–1650.

[32] Du, F., Zhou, J., Gong, R., Huang, X., Pansuria, M., Virtue, A., et al., 2012. Endothelial progenitor cells in atherosclerosis. Frontiers in Bioscience 17:2327–2349.

[33] Lappas, M., 2012. Anti-inflammatory properties of sirtuin 6 in human umbilical vein endothelial cells. Mediators of Inflammation, 597514.

[34] Spagnoli, L.G., Mauriello, A., Sangiorgi, G., Fratoni, S., Bonanno, E., Schwartz, R.S., et al., 2004. Extracranial thrombotically active carotid plaque as a risk factor for ischemic stroke. Journal of the American Medical Association 292:1845–1852.

[35] Moreno, P.R., Murcia, A.M., Palacios, I.F., Leon, M.N., Bernardi, V.H.-, Fuster, V., et al., 2000. Coronary composition and macrophage infiltration in atherectomy specimens from patients with diabetes mellitus. Circulation 102: 2180–2184.

[36] Sinha, B., Ghosal, S., 2019 Apr. Meta-analyses of the effects of DPP-4 inhibitors, SGLT2 inhibitors and GLP1 receptor analogues on cardiovascular death, myocardial infarction, stroke and hospitalization for heart failure. Diabetes Research and Clinical Practice 150:8–16. https://doi.org/10.1016/j.diabres.2019.02.014.

[37] Niccoli, G., Giubilato, S., Di Vito, L., Leo, A., Cosentino, N., Pitocco, D., et al., 2013. Severity of coronary atherosclerosis in patients with a first acute coronary event: a diabetes paradox. European Heart Journal 34:729–741.

